J. Appl. Comput. Mech., 7(2) (2021) 965-969
DOI: 10.22055/JACM.2021.35794.2735

ISSN: 2383-4536
jacm.scu.ac.ir

Shahid Chamran University of Ahvaz

Journal of Applied and Computational Mechanics

Research Paper

# Fatigue Life Analysis of Bus Body based on User Target Load Spectrum

Guangwei Meng[1], Chuanxin Ren[1], Xiaolin Li[2], Liming Zhou[1], Feng Li[1], Tonghui Wei[1]

[1] School of Mechanical and Aerospace Engineering, Jilin University, No.5988, Renmin Street, Changchun, 130025, PR China
[2] College of Construction Engineering, Jilin University, No.6, Ximinzhu Street, Changchun, 130000, PR China

Received November 19 2020; Revised January 14 2021; Accepted for publication January 14 2021.
Corresponding authors: X. Li (lixiaolin@jlu.edu.cn), L. Zhou (lmzhou1982@gmail.com), F. Li (fengli@jlu.edu.cn)


**Abstract.** In this article, fatigue life of a bus body is analyzed based on the user target load spectrum. A finite element model of the bus body is built with characteristics. The static analysis result is obtained by using the inertia release method and a multi-body dynamic model is established by using the rigid flexible coupling method. According to user investigation, the user load spectrum is obtained through dynamic simulation. The average value and amplitude of each level of stress are extracted from the load spectrum information. With the fatigue properties of the material, the damage value of the bus body is determined by using the S-N curve method and Miner linear cumulative damage theory. The simulation gives the fatigue life and damage values of the most dangerous position of the body structure. Calculation shows that the fatigue life of the bus body meets durability requirements.

**Keywords**: Bus body; Rigid-flexible coupling; Inertial release; Fatigue life; Multibody dynamics.

## 1. Introduction

Fatigue analysis is one of the main issues to be considered in engineering. From formal service to scrapping, fatigue damage is one of the major causes for the scrapping of cars, which is mainly induced by the bearing alternating loads of the body in most cases. Areas with stress concentration can result in the appearance of cracks during cyclic loading [1].

Scholars worldwide have extensively studied the fatigue life of automobile bodies. Skorupa [2] made fatigue tests under a range of squeeze force levels and conclude the fatigue behaviour of joints. Some Scholars compared experiments and simulation to effective methods for structural fatigue analysis [3-4]. By applying *ADAMS* into multi-body dynamics simulation on a small passenger car, KIM et al. [5] acquired load time history data based on the principle of rigid-flexible coupling, and then identified the body components with larger fatigue damage through fatigue simulation analysis. Meanwhile, they presented suggestions for improvement and optimization. Xiang [6] used *ABAQUS* to analyze the ultra-low-cycle fatigue (ULCF) life and compare the FE data with experimental results. Vinyas [7-8] used commercial software *COMSOL* to simulate engineering structures to obtain their mechanical properties and compared the results to prove the correctness of the method. Kong [9] simulated on a quarter car and predicted the fatigue life of car coil springs by hybrid multi-layer perceptron artificial neural network (HMLP ANN) models. Kashyzadeh [10] investigated the fatigue life of automotive components under different loading conditions including VAL. Darwich [11] used FEA to compare the fatigue of hip implant stems coated with carbon/PEEK and PEEK. Putra [12] calculated the fatigue life of an automotive coil spring considering road surface roughness and concluded that a road surface as well as driving behaviour affects the car fatigue life significantly. Liu [13] applied the railway vehicles random analysis procedure (RVRAP) to explore the fatigue failure of the rigid-flexibility model. The simulation analysis of the four schemes was established, and the simulation analysis was carried out. In order to verify the results, a real vehicle body structure test was carried out on a shaking table, and the root mean square value of the dynamic stress was obtained and compared with the simulation results. Farrahi [14-15] completed fatigue simulation under different road condition by using a combination of multi-body dynamics and finite element analyses. He considered road roughness and calculate the fatigue life of vehicle body spot weld. Men [16] processed customer data into a target rotating rainflow counting cyclic matrix and eliminates small cyclic loads that have less impact on fatigue life, and then collected the percentage of roads and the data in actual customer surveys to calculate the fatigue damage.

In this article, we predicted the fatigue life of the body with CAE technology on the target load spectrum of users. First, a finite element model of the bus body was established. Then, multi-body dynamics simulation of the bus under different road conditions was performed to simulate its driving condition on actual user target road surface based on rigid-flexible coupling. Finally, the fatigue life of the bus body frame structure was analyzed based on the S-N curve method and Miner linear cumulative damage theory. The analysis results show that the body meets the fatigue life requirements.

Published online: January 17 2021

**Table 1.** User Driving Survey Table

| Road conditions | Level | Average mileage /km | Percentage |
|---|---|---|---|
| Mountain road | B | 25597 | 24.4% |
| Off road | C | 722 | 0.6% |
| Urban road | A | 6693 | 5.6% |
| Smooth road | A | 75829 | 63.4% |
| Middle road | C | 10776 | 9.0% |
| Bad road | C | 2174 | 1.8% |

**Table 2.** Pavement level classification criteria

| Road level | $G_q(n_0)/(10^{-6}m^3)$ | ADAMS/CAR Pavement file setting parameters |
|---|---|---|
| A | 16 | 0.001 |
| B | 64 | 0.002 |
| C | 256 | 0.004 |

## 2. Finite element and multi-body dynamics modeling

There are lots of large-scale advanced numerical simulation softwares that can be used for modeling and analysis such as *ADAMS*, *COMSOL*, *ANSYS*, etc [17-18]. Before the finite element analysis, the model mainly involving quadrilateral shell elements was constructed according to the structural characteristics, and the different components were interconnected by common nodes. The model has 1,206,389 nodes and 1,218,302 elements.

A bus suspension (the rigid part) and the bus body (flexible body) are connected by a connecting body to achieve a rigid-flexible coupling effect. The front and rear suspensions are double-wishbone independent and non-independent suspensions respectively. A rack-and-pinion steering gear and a tire model for durability analysis are used to meet the fatigue analysis under complex working conditions. Finally, the power system is set up and assembled by determining the quality and location of the engine part. Fig. 1 shows the multi-body dynamics model of the bus, including front and rear suspension subsystems, a steering subsystem, front tire and rear tire subsystems, a body subsystem, a manufacturing power subsystem and an engine subsystem.

## 3. User survey

Before calculating the fatigue life of the bus, we conducted a bus usage survey on the user. In the surveys, each user must provide the percentage of mileage on each type of road. User roads can be divided into three types flat roads, medium uneven roads and extremely uneven roads. The requirements for vehicle speed also differ among different road condition. The three road conditions correspond to the three road surface levels respectively, or the road roughness index. According to the survey results of 503 users, the user annual mileage survey is shown in Table 1.

Road unevenness greatly influences the multi-body dynamics analysis of the bus body, and the power spectrum density fitting formula is as follows:

$$G_q(n) = G_q(n_0)\left(\frac{n}{n_0}\right)^{-w} \tag{1}$$

where $n_0$ is the spatial frequency of the reference road surface (generally is 0.1 $m^{-1}$ for a flat road); $n$ is the spatial frequency of the target road surface, $m^{-1}$; $w$ is the frequency index, which is a constant; $G_q(n_0)$ is the coefficient of road roughness. According to the upper and lower limits of the power density and the requirements of *International Standards Association*, the road surface can be divided into 8 levels from A to H.

The power spectrum density is used as the characterization parameter to classify different types of pavements. Here, we mainly adopt A-level, B-level and C-level roads. Flat roads such as expressways and national highways are classified as A-level. Mountain roads are categorized as B-level. Other pavements are regarded as C-level. The standard geometric mean values of the power spectral density $G_q(n_0)$ divided by A-C levels are shown in Table 2.

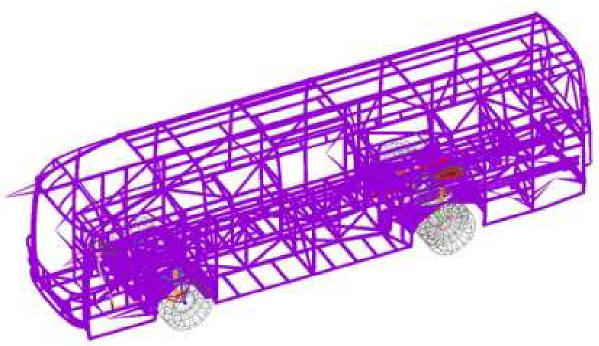

**Fig. 1.** Multi-body Dynamics Model of Bus

## 4. Vehicle dynamics simulation and load spectrum extraction

We simulate the straight-line driving of the bus on A-, B-, and C-level roads separately. According to the actual situation, the bus is running on A-, B-, and C-level roads at speeds of 90 km/h in the 6th gear, 60 km/h in the 4th gear and 40 km/h in the 3rd gear. The simulation time is 30 s, and the number of simulation steps is 300. After the vehicle road simulation, each connection point has three directions of force and torque, and the channel is selected according to the number of connection points to extract the load spectrum. Here is an example of the connection point between the previous suspension shock absorber and the vehicle body. The load spectrum of the x-direction force at this point under a C-level road is shown in Fig. 2(a). Due to space limitations, the calculation results of other connection points will not be listed. According to the rain-flow counting method, the rain-flow histogram generated by the load spectrum is shown in Fig. 2(b) [19].

## 5. Fatigue life analysis

### 5.1 Inertial release method statics analysis

In static analysis, the usual practice is to impose constraints to ensure that the structure does not move. When suitable constraints cannot be applied, the inertial force of the structure can be used to balance the external forces. In this way, static analysis of the structure can be completed without imposing constraints, and the calculation errors caused by the reaction force at the constraints can be eliminated to obtain a more actual calculation result [20-21]. The inertia release analysis is realized in *HyperMesh* by applying a unit load to all the connections between the body and the suspension. As an example of applying unit force in the x-direction at the connection point between the left side of the suspension and the body, the stress cloud diagram of the static analysis results is shown in Fig. 3. The maximum stress is illustrated by the red circle.

### 5.2 Fatigue life analysis of S-N curve method

The S-N curve method of materials considers the relationship between fatigue life and loaded materials, and is a major way to analyze the fatigue life of materials. The S-N curve is usually expressed as follow:

$$S^m N = C \tag{2}$$

where $m$ and $C$ are material parameters.

If the influence of average stress is considered, the fatigue life formula of the structure under the $j$-th stress level is transformed into:

$$N_j = C\left(\frac{S_b}{S_b - S_{m,j}} S_{a,j}\right)^{-m} \tag{3}$$

where $S_{m,j}$ and $S_{a,j}$ are the average stress and stress amplitude of the $j$-th level; $S_b$ is the ultimate strength of the material. The expressions of $S_{m,j}$ and $S_{a,j}$ are:

$$S_{m,j} = \frac{S_{\max,j} + S_{\min,j}}{2} \tag{4}$$

$$S_{a,j} = \frac{S_{\max,j} - S_{\min,j}}{2} \tag{5}$$

where $S_{\max,j}$ and $S_{\min,j}$ are the maximum and minimum stresses of the $j$-th level respectively.

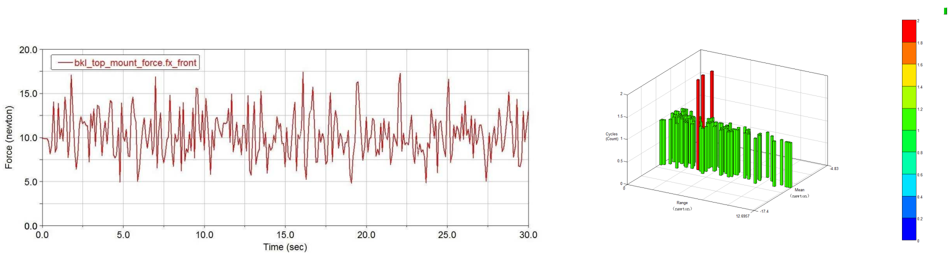


(a) Load spectrum (b) Rain-flow histogram

**Fig. 2.** Front suspension shock absorber and body connection point at C-grade road x-direction force

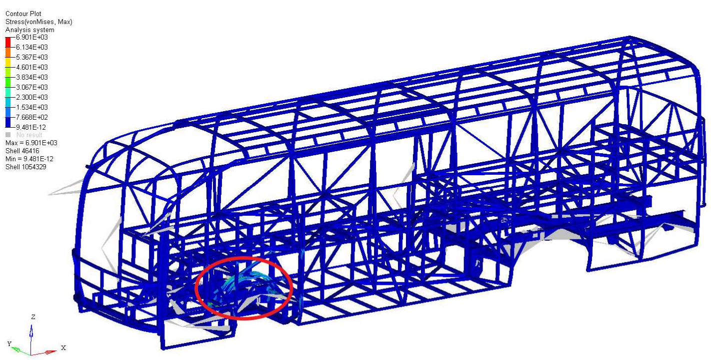


**Fig. 3.** Bus body stress cloud map with x-direction unit force applied to the connection point between the left side of the front suspension and the body

**Table 3.** Dangerous node life damage value

| Road level | Dangerous node ID | Life | Damage |
|---|---|---|---|
| A-level | none | $+\infty$ | none |
| B-level | 654908 | $9.07\times10^{13}$ | $1.103\times10^{-14}$ |
| | 653628 | $2.31\times10^{16}$ | $4.329\times10^{-17}$ |
| C-level | 653628 | $6.189\times10^{12}$ | $1.616\times10^{-13}$ |
| | 654908 | $2.909\times10^{13}$ | $3.437\times10^{-14}$ |

**Table 4.** Percentage of damage to body dangerous points under varying levels of road surface

| Node ID | Road level | | | Damage |
|---|---|---|---|---|
| | A | B | C | |
| 654908 | 0 | $5.74\times10^{-10}$ | $1.44\times10^{-9}$ | $2.014\times10^{-9}$ |
| | 0 | 28.5% | 71.5% | |
| 653628 | 0 | $2.25\times10^{-12}$ | $6.79\times10^{-9}$ | $6.79\times10^{-9}$ |
| | 0 | 0 | 100% | |

According to Miner linear cumulative damage law, when a component is subjected to multi-level loads, the total damage $D$ is [22-25]:

$$D=\sum_{j=1}^{p}\frac{n_j}{N_j} \tag{6}$$

where $n_j$ is the number of cycles under the $j$-th load, $N_j$ is the fatigue life of the bus body corresponding to the $j$-th load, and $p$ is the total number of loads applied. $D > 1$ means fatigue failure occurs.

The simulated mileages under A-, B-, and C-level roads are 0.75, 0.5, and 0.33 km respectively. Through calculation and analysis, the fatigue life and damage value of each element node of the finite element as well as the damage cloud map of the bus body can be obtained. The damage cloud diagram under a C-level road as an example is shown in Fig. 4.

The life value and damage value of the dangerous nodes on the body frame are shown in Table 3.

Based on user goals and according to statistics, the mileages of the bus on A-, B-, and C-levels roads in one year are 83,000, 26,000, and 14,000 km respectively. Thereby, the damage value and percentage of the body frame during simulation on various roads are calculated. The percentages are shown in Table 4.

## 6. Conclusion

It can be predicted from Table 4 that the fatigue life of the bus body frame meets the requirements. For the dangerous point No.654908, the damage of C-level road surface is relatively large, and for the node No.653628, the unevenness of A-level and B-level road surfaces basically contributes zero to the damage of the body frame. These results prove that the road surface level significantly impacts the fatigue performance of the bus. The scrapping standard for automobiles in China provides scrapped driving time of 10 years for buses. According to the 1-year total damage value (Table 4), after 10 years of driving, the total damage values of node No.654908 and No.653628 after 10 years are $2.014\times10^{-8}$ and $6.79\times10^{-8}$, respectively. The total damage values are less than 1, which meet the fatigue requirements. This article provides a method to analyze the fatigue life of the bus body. The load spectrum under the A-, B-, and C-level roads can be obtained through rigid-flexible coupling and multi-body dynamics simulation and the statics results can be obtained using the inertia release method. The parameters required by the S-N curve method can be extracted from these simulation results, so that the fatigue life of the bus body can be calculated. With t Miner linear cumulative damage theory, the fatigue life under the user target road surface obtained from the investigation can be solved.

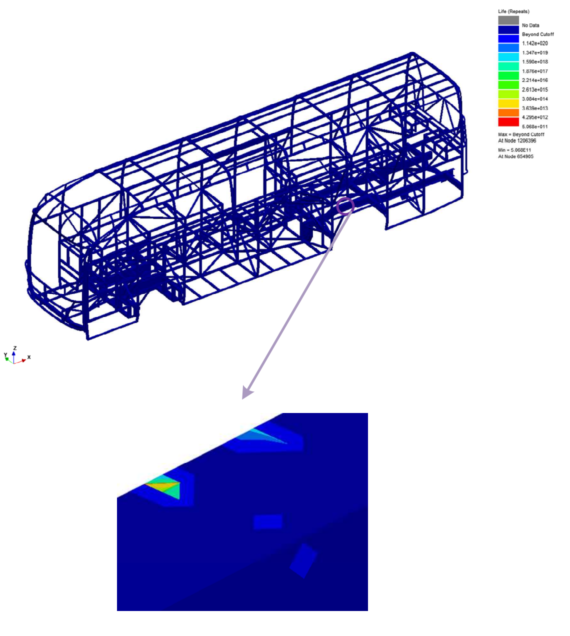

**Fig. 4.** Damage cloud diagram from fatigue analysis of C-level pavement

## Conflict of Interest

The authors declared no potential conflicts of interest with respect to the research, authorship, and publication of this article.

## Funding

This work was supported by Jilin Provincial Department of Education (grant number JJKH20190131KJ), Jilin Provincial Department of Education (grant no. JJKH20200952KJ), National Natural Science Foundation of China (grant no. 51975243).

## References

[1] U. TATIĆ, K. ČOLIĆ, A. SEDMAK, Ž. MIŠKOVIĆ, A. PETROVIĆ, Evaluation of the Locking Compression Plates Stress-Strain Fields, *Technical Gazette*, 25(1) (2018) 112-117.
[2] M. Skorupa, A. Skorupa, T. Machniewicz, A. Korbel, Effect of production variables on the fatigue behaviour of riveted lap joints, *International Journal of Fatigue*, 32 (2010) 996-1003.
[3] X. Li, J. Fang, Q. Zhang, S. Zhao, X. Guan, Study on Key Technology of Railway Freight Car Body Fatigue Test, *Journal of Falure Analysis and Prevention*, 20 (2020) 261-269.
[4] Y. Liu, F. Dai, L. Dong, N. Xu, P. Feng, Experimental Investigation on the Fatigue Mechanical Properties of Intermittently Jointed Rock Models Under Cyclic Uniaxial Compression with Different Loading Parameters, *Rock Mechanics and Rock Engineering*, 51 (2018) 47-68.
[5] H.S. Kim, H.J. Yim, C.B. Kim, Computational durability prediction of body structures in prototype vehicles, *International Journal of Automotive Technology*, 3(4) (2002) 129-35.
[6] P. Xiang, Z. Qing, L.-J. Jia, M. Wu, J. Xie, Damage evaluation and ultra-low-cycle fatigue analysis of high-rise steel frame with mesoscopic fracture models, *Soil Dynamics and Earthquake Engineering*, 139 (2020) 106283.
[7] M. Vinyas, A.S. Sandeep, T. Nguyen-Thoi, F. Ebrahimi, D.N. Duc, A finite element–based assessment of free vibration behaviour of circular and annular magneto-electro-elastic plates using higher order shear deformation theory, *Journal of Intelligent Material Systems and Structures*, 30(16) (2019) 2478-2501.
[8] M. Vinyas, K.K. Sunny, D. Harursampath, T. Nguyen-Thoi, M.A.R. Loja, Influence of interphase on the multi-physics coupled frequency of threephase smart magneto-electro-elastic composite plates, *Composite Structures*, 226(2019) 111254.
[9] Y.S. Kong, S. Abdullah, D. Schramm, M.Z. Omar, S.M. Haris, Optimization of spring fatigue life prediction model for vehicle ride using hybrid multi-layer perceptron artificial neural networks, *Mechanical Systems and Signal Processing*, 122(2019) 597-621.
[10] K.R. Kashyzadeh, Effects of Axial and Multiaxial Variable Amplitude Loading Conditions on the Fatigue Life Assessment of Automotive Steering Knuckle, *Journal of Failure Analysis and Prevention*, 20 (2020) 455–463.
[12] T.E. Putra, Husaini, M.N. Machmud, Predicting the fatigue life of an automotive coil spring considering road surface roughness, *Engineering Failure Analysis*, 116 (2020) 104722.
[13] X. Liu, Y. Zhang, S. Xie, Q. Zhang, H. Guo, Fatigue failure analysis of express freight sliding side covered wagon based on the rigid-flexibility model, *International Journal of Structural Integrity*, 2019, DOI: 10.1108/IJSI-11-2019-0122.
[14] G.H. Farrahi, A. Ahmadi, K.R. Kasyzadeh, Simulation of vehicle body spot weld failures due to fatigue by considering road roughness and vehicle velocity, *Simulation Modelling Practice and Theory*, 105 (2020) 102168.
[15] G.H. Farrahi, K.R. Kashyzadeh, M. Minaei, A. Sharifpour, S. Riazi, Analysis of Resistance Spot Welding Process Parameters Effect on the Weld Quality of Three-steel Sheets Used in Automotive Industry: Experimental and Finite Element Simulation, *International Journal of Engineering*, 33(1) (2020) 148-157.
[16] Y. Men, H. Yu, H. Yu, Development of block loading spectrum for car powertrain rig test correlated with customers' usage, *Advances in Mechanical Engineering*, 9(9) (2017) 1-10.
[17] M. Vinyas, On frequency response of porous functionally graded magneto-electroelastic circular and annular plates with different electro-magnetic conditions using HSDT, *Composite Structures*, 240 (2020) 112044.
[18] M. Vinyas, A higher-order free vibration analysis of carbon nanotube-reinforced magneto-electro-elastic plates using finite element methods, *Composites Part B*, 158 (2019) 286-301
[19] A.S. SENER, Fatigue Life Resolution of the Steering Wheel Tie Rod of a LCV with FEA, *Mechanika*, 23(5) (2017) 622-629.
[20] A. Ahmadi, G.H. Farrahi, A comparative study on the fatigue life of the vehicle body spot welds using different numerical techniques: Inertia relief and Modal dynamic analyses, *Frattura ed Integrità Strutturale*, 52 (2020) 67-81.
[21] C.-J. Thore, Topology optimization of freely floating elastic continua using the inertia relief method, *Computer Methods in Applied Mechanics and Engineering*, 361 (2020) 112733.
[22] Y. Ma, A. Peng, L. Wang, C. Zhang, J. Li, J. Zhang, Fatigue performance of an innovative shallow-buried modular bridge expansion joint, *Engineering Structures*, 221 (2020) 111107.
[23] S. Chen, K. Xu, X. Zheng, J. Li, B. Fan, X. Yao, Z. Li, Linear and nonlinear analyses of normal and fatigue heart rate variability signals for miners in high-altitude and cold areas, *Computer Methods and Programs in Biomedicine*, 196 (2020) 105667.
[24] S. Wang, X. Liu, C. Jiang, X. Wang, X. Wang, Prediction and evaluation of fatigue life for mechanical components considering an elasticity-based load spectrum, *Fatigue & Fracture Engineering Materials & Structures*, 2020, DOI: 10.1111/ffe.13340.
[25] C. Jiang, X. Liu, X. Wang, X. Wang, S. Su, Interval dynamic reliability analysis of mechanical components under multistage load based on strength degradation, *Quality Reliability Engineering International*, 2020, DOI: 10.1002/qre.2749.

## ORCID iD

Guangwei Meng https://orcid.org/0000-0001-7880-4648
Chuanxin Ren https://orcid.org/0000-0001-7424-7805
Xiaolin Li https://orcid.org/0000-0001-8044-3634
Liming Zhou http://orcid.org/0000-0002-5238-3803
Feng Li https://orcid.org/0000-0001-5602-0017
Tonghui Wei https://orcid.org/0000-0003-4013-2975



How to cite this article: Meng G. et al., Fatigue Life Analysis of Bus Body based on User Target Load Spectrum, *J. Appl. Comput. Mech.*, 7(2), 2021, 965–969. https://doi.org/10.22055/JACM.2021.35794.2735